Rogue Wave Statistics and Dynamics Using Large-Scale Direct Simulations

Dick K.P. Yue
Center for Ocean Engineering
Department of Mechanical Engineering
Massachusetts Institute of Technology
Cambridge, MA 02139
phone: (617) 253- 6823 fax: (617) 258-9389 email: yue@mit.edu

Yuming Liu
Department of Mechanical Engineering
Massachusetts Institute of Technology
Cambridge, MA 02139
phone: (617) 252- 1647 fax: (617) 258-9389 email: yuming@mit.edu

Award Number: N00014-06-1-0278
http://www.mit.edu/~vfrl/

LONG-TERM GOAL

The long-term goal is to study the generation mechanisms and evolution dynamics of rogue waves using large-scale three-dimensional nonlinear phase-resolved wavefield simulations and to establish the foundation for future development of effective tools for prediction of rogue wave occurrences in realistic ocean wave environments.

OBJECTIVES:

The specific scientific and technical objectives are to:

- Obtain a significant number of representative large-scale rogue wave datasets using direct simulations
- Verify the validity and limitations of existing theories and models for the statistics of large-amplitude wavefields and the occurrence of rogue waves
- Understand the fundamental mechanisms for rogue wave development. Of particular importance is to validate (or invalidate) the hypotheses and assumptions underlying the existing theories, statistics and models/tools for rogue wave prediction
- Elucidate the evolution kinematics and dynamics of rogue wave events

APPROACH

The objectives stated above are achieved in a coordinated effort involving three major activities: (I) Development of a significant number of large-scale computations and datasets for nonlinear evolution of wavefields for different initial wavefield (spectral) parameters and environmental/boundary conditions; (II) Use of direct computations to quantitatively verify and validate existing theories and

Report Documentation Page

Form Approved
OMB No. 0704-0188

1. REPORT DATE	2. REPORT TYPE	3. DATES COVERED
30 SEP 2006		**00-00-2006 to 00-00-2006**

4. TITLE AND SUBTITLE	5a. CONTRACT NUMBER
Rogue Wave Statistics and Dynamics Using Large-Scale Direct Simulations	5b. GRANT NUMBER
	5c. PROGRAM ELEMENT NUMBER
6. AUTHOR(S)	5d. PROJECT NUMBER
	5e. TASK NUMBER
	5f. WORK UNIT NUMBER
7. PERFORMING ORGANIZATION NAME(S) AND ADDRESS(ES) **Massachusetts Institute of Technology,Department of Mechanical Engineering,77 Massachusetts Avenue,Cambridge,MA,02139**	8. PERFORMING ORGANIZATION REPORT NUMBER
9. SPONSORING/MONITORING AGENCY NAME(S) AND ADDRESS(ES)	10. SPONSOR/MONITOR'S ACRONYM(S)
	11. SPONSOR/MONITOR'S REPORT NUMBER(S)

12. DISTRIBUTION/AVAILABILITY STATEMENT
Approved for public release; distribution unlimited

13. SUPPLEMENTARY NOTES

14. ABSTRACT

15. SUBJECT TERMS

16. SECURITY CLASSIFICATION OF:			17. LIMITATION OF ABSTRACT	18. NUMBER OF PAGES	19a. NAME OF RESPONSIBLE PERSON
a. REPORT **unclassified**	b. ABSTRACT **unclassified**	c. THIS PAGE **unclassified**	**Same as Report (SAR)**	**7**	

models for wavefield statistics and the hypotheses on rogue wave formation; and (III) Use of these computations to systematically investigate the stochastic and deterministic mechanisms underlying the occurrence of rogue wave events and to characterize the statistical and physical properties of such events.

For the large-scale computations, we apply the direct phase-resolved **s**imulations of **n**onlinear **o**cean **w**avefields (SNOW). SNOW is developed based on a high-order spectral method (Dommermuth & Yue 1987; Tsai & Yue 1996), which resolves the phase of a large number of wave modes and accounts for their nonlinear interactions up to an arbitrary high order M including broadband non-resonant and resonant interactions up to any specified order. SNOW achieves an exponential convergence and a (near) linear computational effort with respect to the number of wave modes N and the interaction order M, and has high scalability on high-performance parallel computing platforms. Unlike phase-averaged and model-equation-based approaches, the present phase-resolved simulation accounts for physical phase-sensitive effects in a direct way. These include the initial distribution of wave phases in the wavefield specified by wave spectrum (which is known to affect the nonlinear evolution); energy dissipation due to wave breaking; and input due to wind forcing.

From the direct simulation, we obtain datasets of wave elevation and kinematics of the complete wavefield during its evolution. By analyzing these datasets, we can determine the statistics of the wavefield, identify rogue wave events, compute the statistics of rogue waves, study the development of rogue waves and groups, and understand details of the rogue wave dynamics.

WORK COMPLETED

- Investigated the validity of the existing classical theories and model equations for the prediction of linear and nonlinear wave statistics under general wave conditions

- Performed a number of computations for large-scale phase-resolved nonlinear wavefield evolution from which we obtained a collection of rogue wave data set for wavefields with different spectral parameters

- Analyzed the characteristics of rogue wave statistics, the mechanisms of rogue wave event development, and the kinematics and dynamics of rogue wave events

- Developed an effective adaptive approach for the account of fully nonlinear effects of local steep waves in the phase-resolved computations of large-scale wavefield evolution

RESULTS

Three main results are presented below: (I) direct comparisons of kurtosis evolution of long- and short-crested wavefields between direct simulations, wave basin experiments, and NLS predictions; (II) comparisons of exceeding probability of wave height of nonlinear ocean wavefields between direct simulations and field measurements; and (III) sample rogue wave events identified in the evolution of nonlinear short-crested ocean wavefields with various wave spectrum parameters.

(I) Evolution of wave elevation kurtosis of nonlinear long- and short-crested ocean wavefields.
Figure 1 shows the comparisons between direct SNOW simulations and wave basin measurements and

NLS model equation predictions for wave elevation kurtosis evolution of both long- and short-crested wavefields. The initial wavefields are generated from JONSWAP spectra. For long-crest waves, two types of wavefields are considered, which have the same peak wavelength λ=3.5m and Phillips parameter α=0.0135, but different enhancement factor γ=6 and γ=1. In SNOW simulations, nonlinear order M=4 and number of wave modes N=4096 are used. In the narrowband case (γ=6), as shown in figure 1a, both *SNOW* simulation and NLS prediction (Onorator *et al.* 2005) agree with the experimental measurements (Onorator *et al.* 2005) well up to x=70m (=20λ). But for x>70m, the *SNOW* simulation compares to the experiment much better than the NLS prediction. In the broadband case (γ=1), figure 1b, the *SNOW* simulation agrees well with the experiments while the NLS prediction deviates significantly from the experiment since the start of the evolution. This is not surprising since unlike NLS, *SNOW* simulations account for broadband wave interactions and high-order nonlinearity. For short-crested waves, there is no available experimental measurement. We make comparisons of the SNOW simulations with the NLS predictions (Socquet-Juglard *et al* 2005) for three different wavefields: (A) γ=5, α=0.01326, and angular spreading width Θ=16°; (B) γ=5, α=0.01326, and Θ=40°; and (C) γ=3.3, α=0.01620, and Θ=80°. In SNOW simulations, M=3 and N=4096×4096 are used. As shown in figure 1c, for the narrowband and narrow spreading case (wavefield A), the SNOW simulation and the NLS prediction agree with each other up to ~ 20Tp (Tp: peak wave period) and then deviate largely afterwards. As the frequency band and/or angular spreading become broader (wavefields B and C), the *SNOW* simulation results differ significantly from the NLS prediction since the very beginning of the evolution of wavefields. These comparisons indicate that the direct SNOW simulations can reliably predict the kurtosis in nonlinear evolution of both long- and short-crested wavefields.

(II) Exceeding probability of wave height in nonlinear ocean wavefields. According to the classical theory, the exceeding probability of wave height, crest height, and trough depth are all given by Rayleigh distributions for infinitely narrow spectrum. How the wave nonlinearity and spectrum bandwidth affect the exceeding probability of wave height is of scientific interest and practical importance. To answer this question, we perform the direct SNOW simulations of long-created wavefield evolution including broadband wavenumber and high-order nonlinearity effects. In the simulation, the initial wavefield is generated from JONSWAP spectra with peak wavelength λ=3.5m, Phillips parameter α=0.0135, and enhancement factor γ=6. This corresponds to a significant wave height of Hs=0.165m and effective wave steepness of 0.15. The statistical results are obtained based on a Monte-Carlo simulation of 100 SNOW computations with the initial wavefields generated from the same spectrum but with different random wave-component phases. The probability distributions of wave height at two moments, t=0 and 120Tp, are plotted in figure 2a, where the Rayleigh distribution is also plotted for comparison. It shows that for the linear wavefield at t=0, Rayleigh distribution overpredicts the wave height probability due to the ignorance of the finite bandwidth effect. For the nonlinear wavefield at t=120Tp, Rayleigh distribution underpredicts the occurring probability of large waves with H/Hs > 2.1. This result, obtained from the direct SNOW simulations, agrees qualitatively well with the field measurements (Mori *et al*. 2002), shown in figures 2b and 2c. The two field observations also show that Rayleigh distribution underpredicts the occurring probability of large waves with crest height bigger than Hs (Hs=4ηrms).

(III) Typical rogue waves identified in the evolution of short-crested nonlinear ocean wavefields. In order to understand the mechanisms of rogue wave development and study the kinematics/dynamics of rogue waves, we performed a large number of large-scale SNOW simulations of nonlinear short-created wavefield evolution. From these simulations, we identified a large collection of rogue wave

events. Four sample rogue waves are shown in figure 3. The plotted area is only a small part of the whole computational domain that is around the rogue wave event. In general, the local wave height of rogue waves is higher for narrower wave spectra while the crest width of rogue waves is larger for narrower spreading.

IMPACT/APPLICATIONS

Proper understanding and prediction of rogue wave events in realistic ocean environments is of critical importance to the design of surface ships and safety of naval operations and ocean explorations. The outcome of this research will establish the necessary foundation for the development of effective rogue wave prediction tools.

REFERENCES

1. Dommermuth, D.G. & Yue, D.K.P. 1988 The nonlinear three-dimensional waves generated by a moving surface disturbance, *Proc. of 17th Symp. on naval hydro*., The Hague, The Netherlands.

2. Mori, N., Liu, P.C. & Yasuda, T. 2002 Analysis of freak wave measurements in the Sea of Japan, *Ocean Engineering*, **29**, 1399-1414.

3. Onorato M., Osborne, A.R., Serio, M. & Cavaleri, L. 2005 Modulation instability and non-Gaussian statistics in experimental random water-wave trains. *Physics of Fluids*. **17**, 078101.

4. Socquet-Juglard, H., Dysthe, K., Trulsen, K., Krogstad, H.E., and Liu, J., 2005 "Probability distribution of surface gravity waves during spectral changes", *J. Fluid Mech.*, **542**, 195-216.

5. Tsai, W. and Yue, D.K.P., Computation of nonlinear free-surface flows, *Ann. Rev. Fluid. Mech.*, Vol. 28, 249-278, 1996.

PUBLICATIONS

1. Wu, G., Liu, Y. & Yue, D.K.P. "Direct Phase-Resolved Simulations of Large-Scale Nonlinear Ocean Wavefields", Proceedings of the DoD HPCMP Users Group Conference 2006, Jun. 26-29, 2006, Denver, CO.

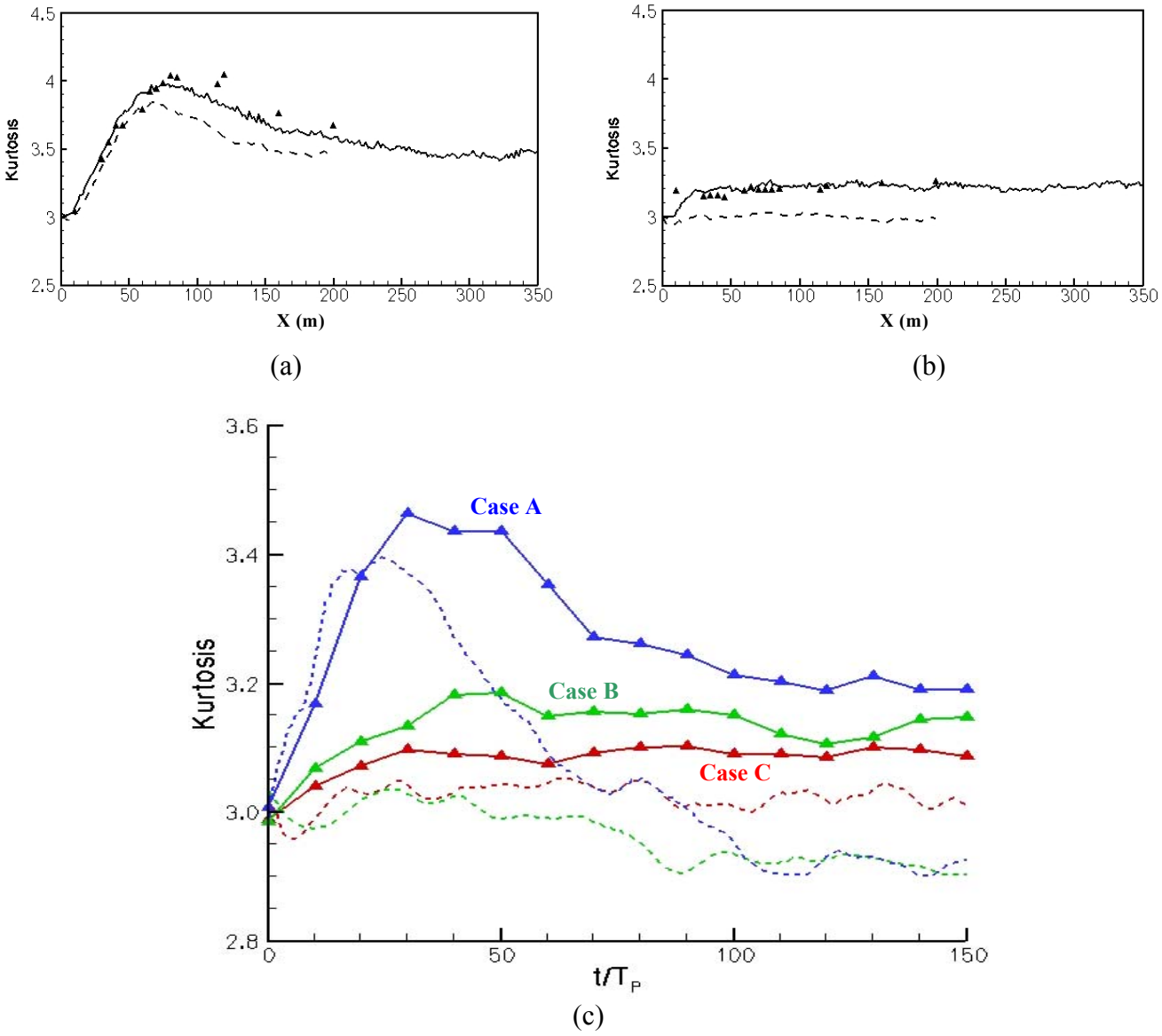

Figure 1: Comparisons among direct SNOW computations, wave basin experiments, and NLS model equation predictions of wave elevation kurtosis in the evolution of nonlinear long-crested wavefields, (a) and (b), and short-crested wave-fields, (c). The initial wavefields are generated from JONSWAP spectra. For long-crest waves, peak wavelength λ=3.5m, Phillips parameter α=0.0135, and enhancement factor γ=6 for (a) and γ=1 for (b). The plots in (a) and (b) are the variation of kurtosis as a function of distance from the wave maker obtained from SNOW simulations (——), experiments (▲, Onorato et al 2005), and NLS model equation (- - - -, Onorato et al. 2005). The plots in (c) are the variation of kurtosis as a function of evolution time obtained from SNOW simulations (—▲—) and NLS model equation (- - - -, Socquet-Juglard et al. 2005) for three different wavefields: (A) γ=5, α=0.01326, and angular spreading width Θ=16° (Blue); (B) γ=5, α=0.01326, and Θ=40° (Green); and (C) γ=3.3, α=0.01620, and Θ=80° (Red).

.

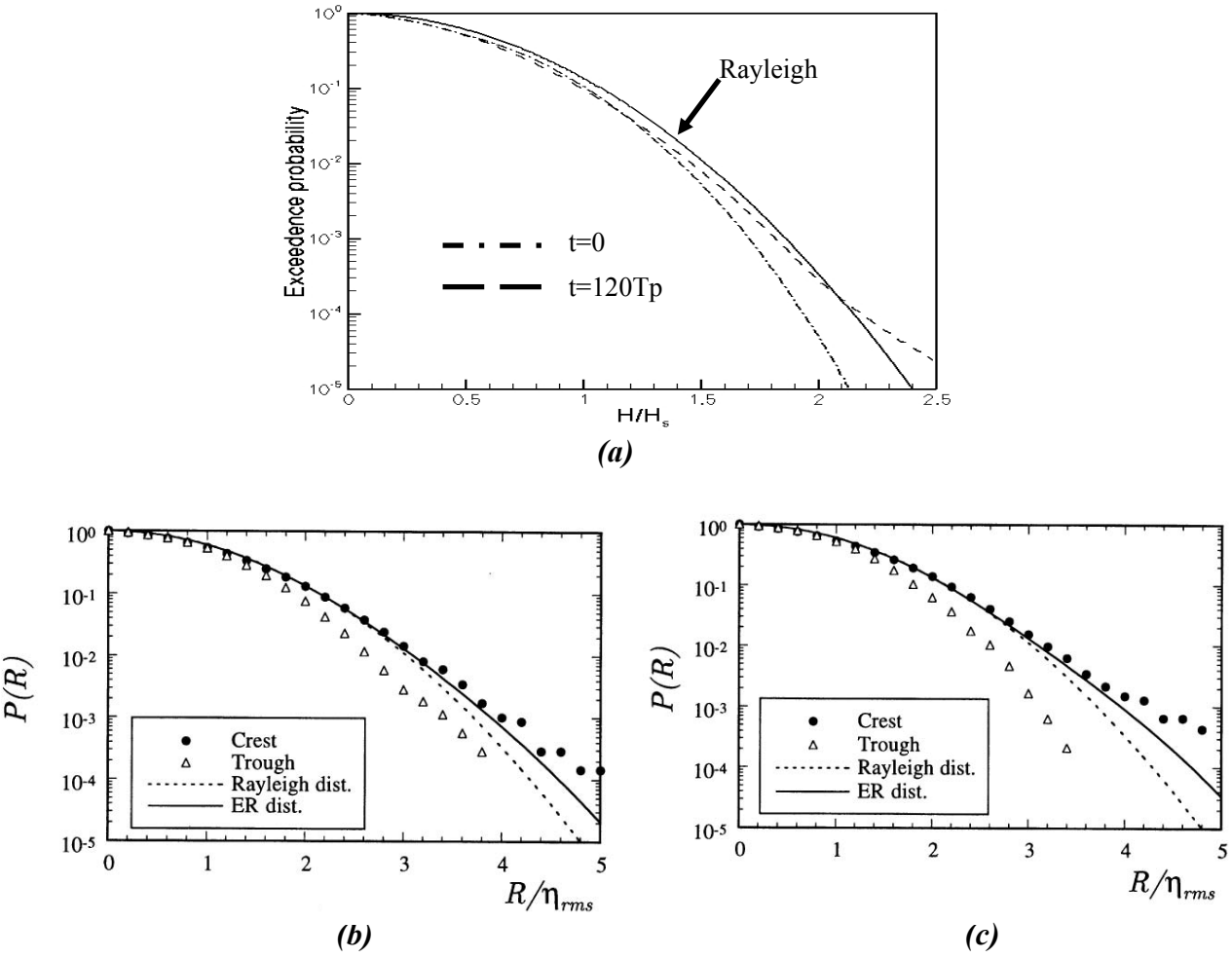

Figure 2: Comparison of exceeding probability of wave height of long-crested nonlinear ocean wavefields between the direct SNOW simulations (a) and the field measurements of Mori et al. (2002), (b) and (c). For the direct SNOW simulations, the initial wavefields are generated from JONSWAP spectra with peak wavelength λ=3.5m, Phillips parameter α=0.0135, and enhancement factor γ=6. The statistical results are obtained based on a Monte-Carlo simulation of 100 runs with initial wavefields generated from the same spectrum but with different random wave-component phases. The plotted in (a) are the Rayleigh distribution (——), the direct SNOW simulation result at t=0 (— - —) and at t=120Tp (- - - -). For the field observations (Mori et al. 2002), characteristic wave period is T1/3=10.25s and characteristic wave steepness is (ka)1/3=0.106 for (b) and T1/3=10.49s and (ka)1/3=0.129 for (c). The plotted in (b) and (c) are: measured crest distribution (•), trough distribution (Δ), Rayleigh distribution (- - - -), and Edgeworth-Rayleigh distribution (——). In the figures, ηrms=Hs/4.

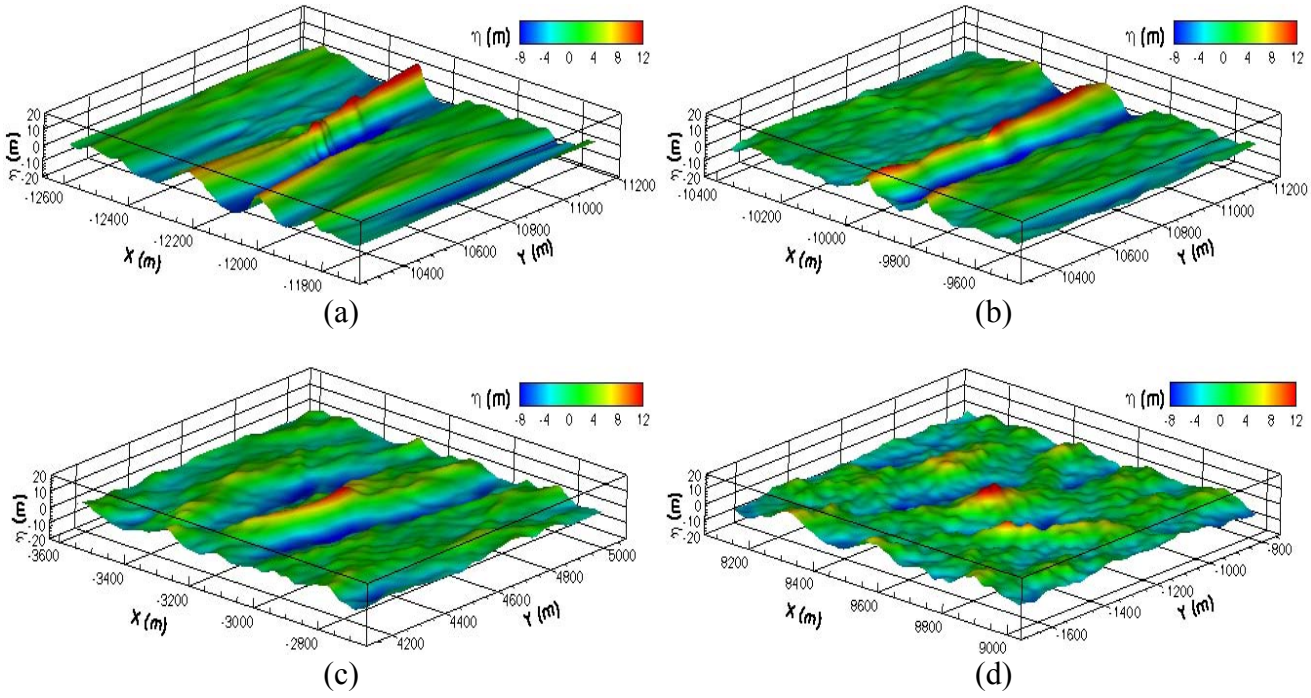

Figure 3: Typical rogue wave events identified from the direct SNOW simulations of short-crested nonlinear ocean wavefield evolution with various spectral parameters. The initial wavefields in the SNOW simulations are all generated from JONSWAP spectra with peak wave period Tp=12sec. Other spectrum parameters are: (a) enhancement factor γ=5, Phillips parameter α=0.01326, and angular spreading width Θ=16°; (b) γ=5, α=0.01326, and Θ=40°; (c) γ=3.3, α=0.01620, and Θ=80°; and (d) γ=3.3, α=0.01620, and Θ=180°. The plotted wavefield is only a small part (0.9km×0.9km) of the whole computational domain (30km×30km). The wave height ratios H/Hs (with Hs =10m) in these rogue wave events are respectively: (a) 3.5; (b) 3.0; (c) 2.4; and (d) 2.5. In SNOW simulations, nonlinear order M=3, and number of wave modes N=4096×4096.